Spiro donor-acceptor TADF emitters: Naked TADF free from inhomogeneity caused by donor acceptor bridge bond disorder. Fast rISC and invariant photophysics in solid state hosts.

AUTHORS

Larissa Gomes Franca, Andrew Danos and Andrew Monkman*

OEM Research group, Department of Physics, Durham University, South Road, Durham, DH1 3LE, United Kingdom.

Supplementary Information:

1. Experimental Details:

a. Sample Preparation:

The solid state samples were fabricated by drop casting onto transparent sapphire substrates and dried in vaccum. All ACRSA:host drop casted films were produced at 1% w/w and 10% w/w ACRSA in host matrix (Zeonex, DPEPO (bis[2-(diphenylphosphino)phenyl]ether oxide),), UGH (m-bis(triphenylsilyl)benzene)). For neat drop casted film, solution of 1 mg/mL were dropped onto substrate.

b. Photophysical characterisation:

Absorption spectra for all films and solutions were collected using a double beam Shimadzu UV-3600 UV/VIS/NIR spectrophotometer. Steady state photoluminescence spectra were measured using both Jobin-Yvon Fluoromax-4 and Fluorolog spectrophotometers.

c. Time-resolved Photoluminescence:

Time-resolved photoluminescence spectra and decays were measured using nanosecond gated spectrograph-coupled iCCD (Stanford) and an Nd:YAG laser emitting at 355 nm or N_2 laser at 337 nm as an excitation sources, in conjunction with a gated 4 Picos iCCD camera. Lifetimes were obtained from a kinetic decays by fitting with a multiexponential function.

2. Experimental energy level scheme derived for ACRSA using nomenclature used by Lyskov and Marian.

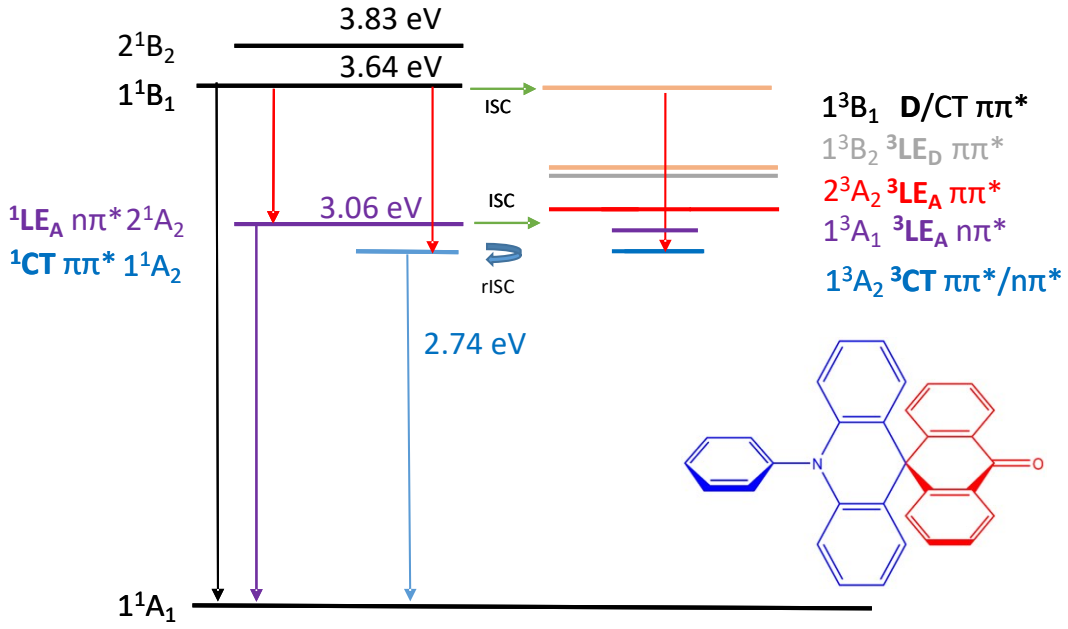

Scheme S1. Experimentally determined excited states of ACRSA measured in toluene[1]. State nomenclature after Lyskov and Marian[2] for consistency. Chemical structure of 10-phenyl-10H,10'H-spiro[acridine-9,90-anthracen]-10'-one (ACRSA) shown in the inset.

Briefly summarising our previous experimental solution state measurements, we find a very strong 1^1B_1 exciton absorption below 350 nm, excitation of which gives rise to fast emission from this high energy excitonic singlet state associated with the donor acridine unit, in competition with internal conversion to two lower lying singlet states of A_2 symmetry and so formally one-photon forbidden states. However, both 2^1A_2 local acceptor ^{1}nπ* (hereafter ^{1}LE) and 1^1A_2 ^{1}ππ* CT (hereafter ^{1}CT) singlet states do have weak direct absorption transitions. Excitation of these states either directly (excitation of 355 nm) or via the upper 1^1B_1 state (excitation 337 nm) gives rise to prompt emission from both A_2 states, simultaneously. ACRSA thus emits from three independent excited states and can be considered one of the most anti-Kasha systems reported. The main deactivation pathway from the 1^1B_1 exciton state is however

via ISC to upper triplet states. These undergo IC to the lowest triplet states that leads to delayed fluorescence (DF) through rISC to the ^{1}CT singlet. The ^{1}LE state decays rapidly by efficient ISC to the local $^3\pi\pi^*$ triplet state by an allowed $^1n\pi^*$ to $^3\pi\pi^*$ transition. This also results in eventual DF from the ^{1}CT state (only), where the lowest energy triplet state, $^3n\pi^*$ local triplet, acts as the mediator triplet for the non-adiabatic vibronic coupling rISC step.[3,4] We find that the main vibronic coupling mode is the anthracenone C=O bond vibration.

3. Molecular structures of host materials

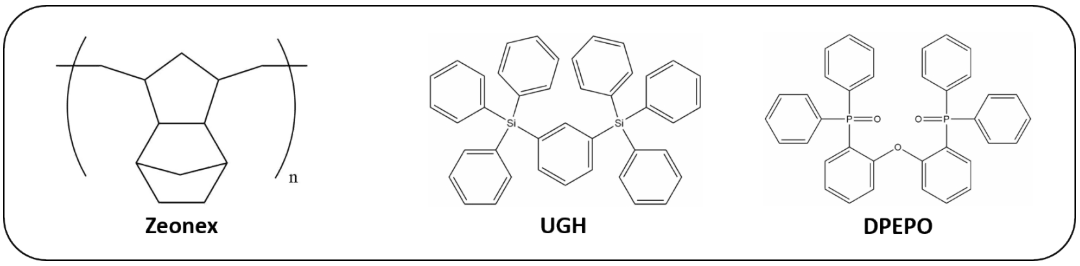

Figure S1. Molecular structures of host materials used in this work.

4. Excitation dependent steady state measurements of 1%wt loading films:

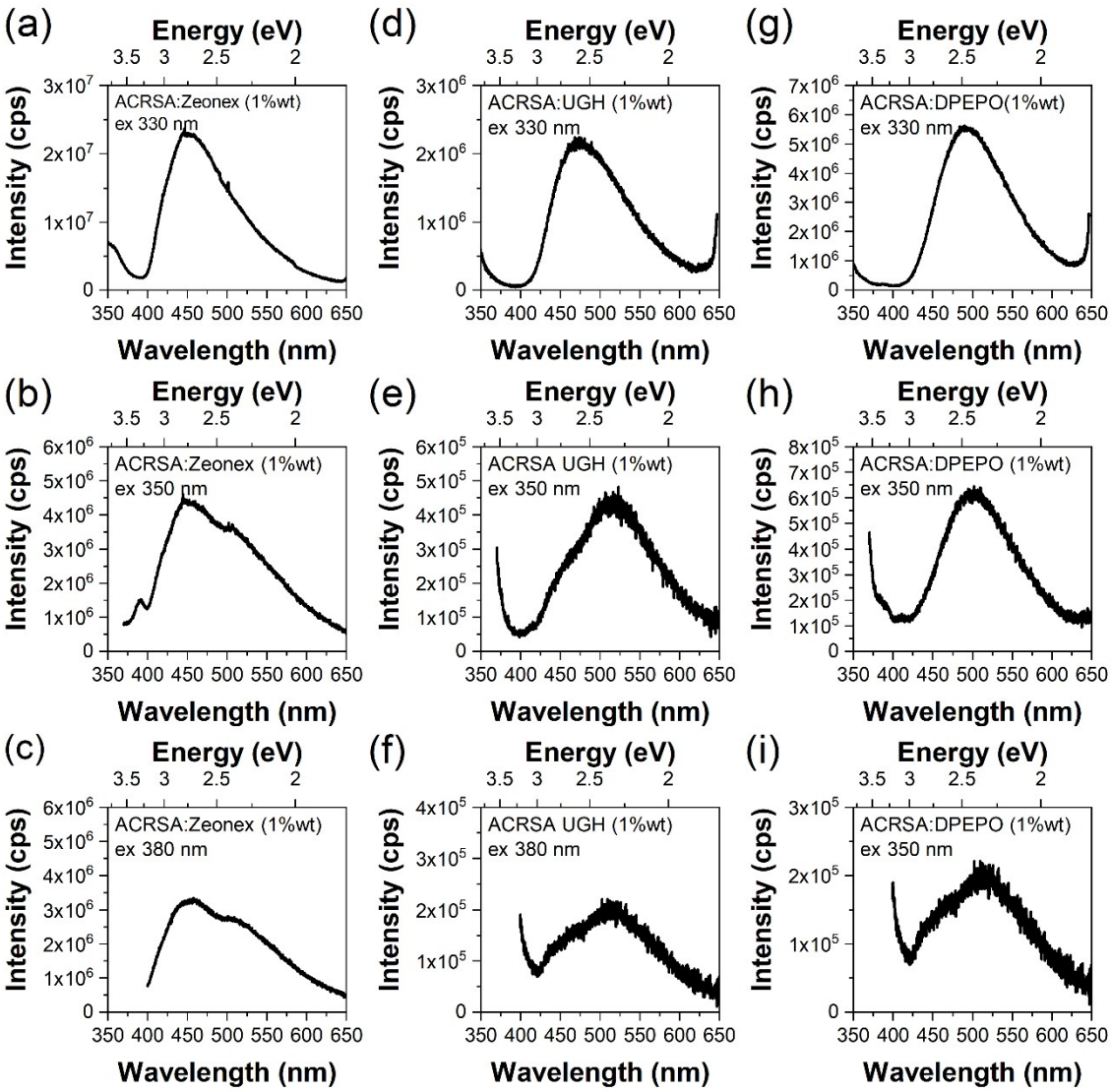

Figure S2. Excitation wavelength dependent steady state emission from ACRSA dispersed in Zeonex (a-c), UGH (d-f) and DPEPO (g-i) at 1%wt loading, measured at room temperature in air.

5. Steady state measurements in vacuum

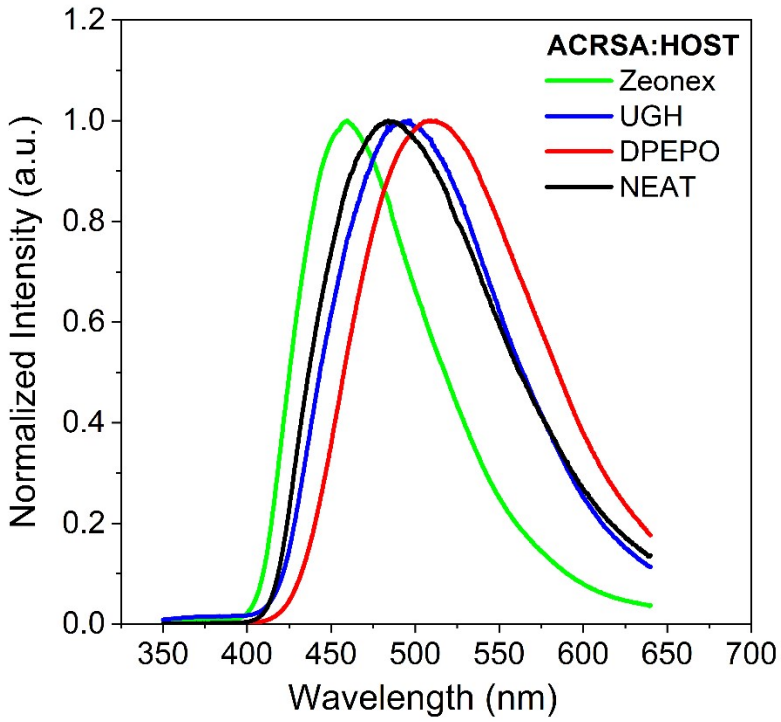

Figure S3. The steady state emission spectra of ACRSA in various host and neat films. Measurements of thin ACRSA:host (10% loading in DPEPO and UGH, 1% in zeonex) and neat ACRSA film made in vacuum and so are dominated by CT emission. Excitation wavelength 330 nm.

6. Fittings of kinetic decay results of ACRSA:Zeonex (1%wt loading) at room temperature and 80 K, with 355 nm excitation wavelength:

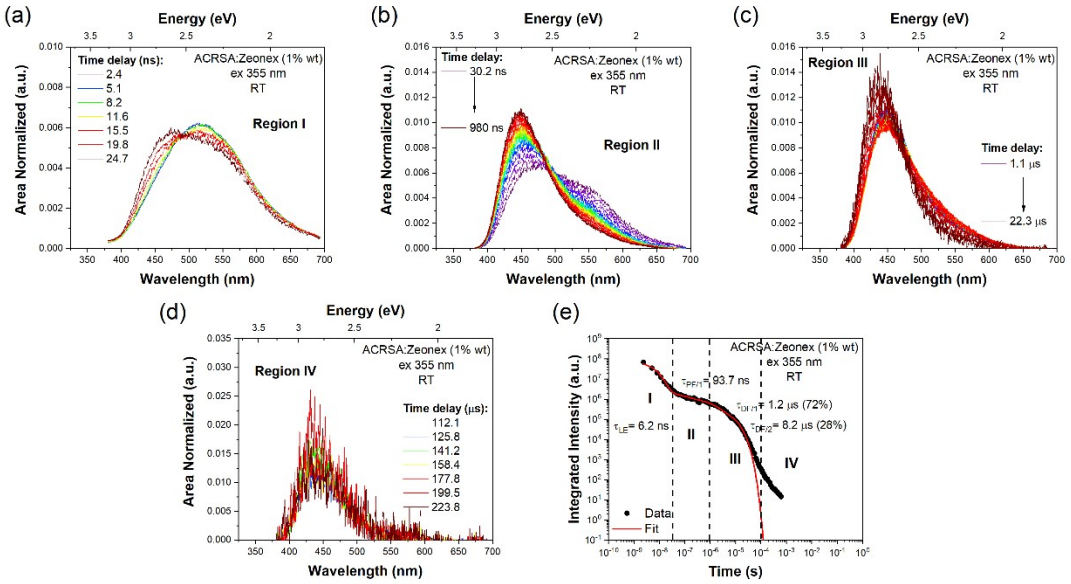

Figure S4. (a)-(d) Area normalised time resolved spectra of ACRSA in zeonex (1% wt), shown in the four main regimes indicated in (e). (e) Fitting of kinetic decay results at room temperature. Laser excitation at 355 nm. Data is tabulated in **Table 1**.

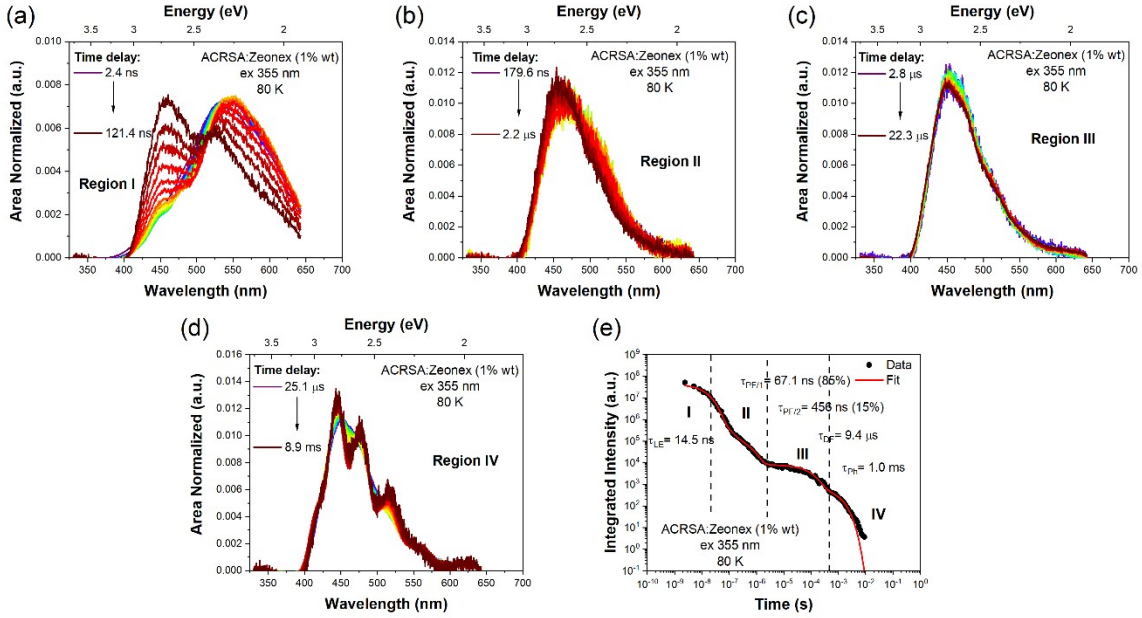

Figure S5. (a)-(d) Area normalised time resolved spectra ACRSA in zeonex (1% wt), shown in the four main regimes indicated in (e). (e) Fitting of kinetic decay results at 80 K. Laser excitation at 355 nm. Data is tabulated in **Table S2**.

7. Fittings of kinetic decay results of ACRSA in UGH and DPEPO (1% wt loading) at 80 K, with 355 nm excitation wavelength:

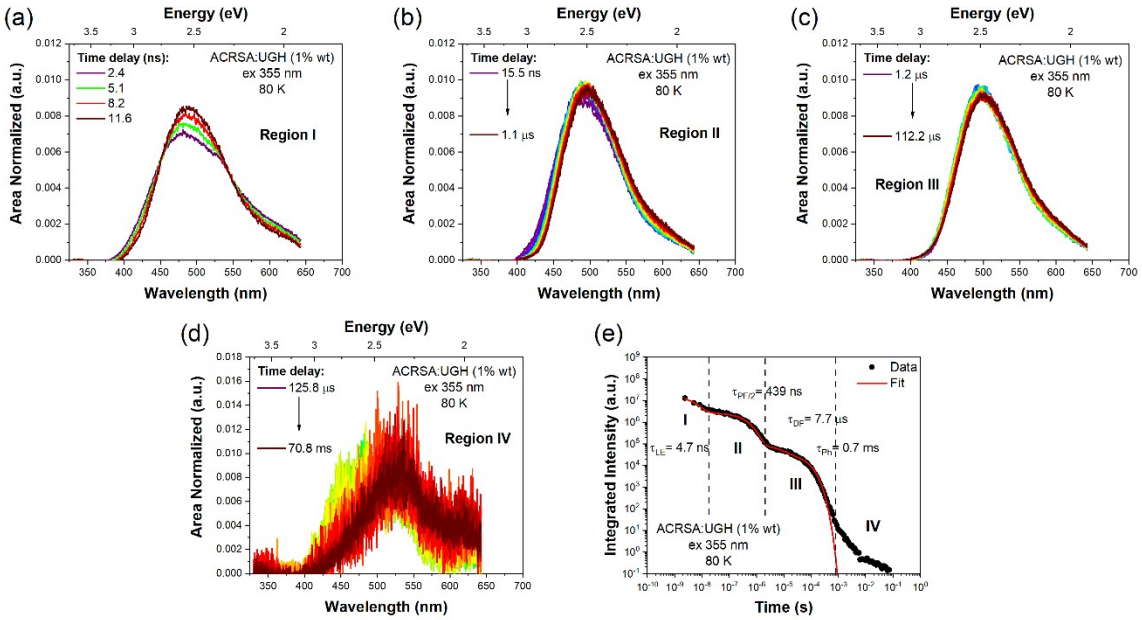

Figure S6. (a)-(d) Area normalised time resolved spectra ACRSA in UGH (1% wt), shown in the four main regimes indicated in (e). (e) Fitting of kinetic decay results at 80 K. Laser excitation at 355 nm. Data is tabulated in **Table S2**.

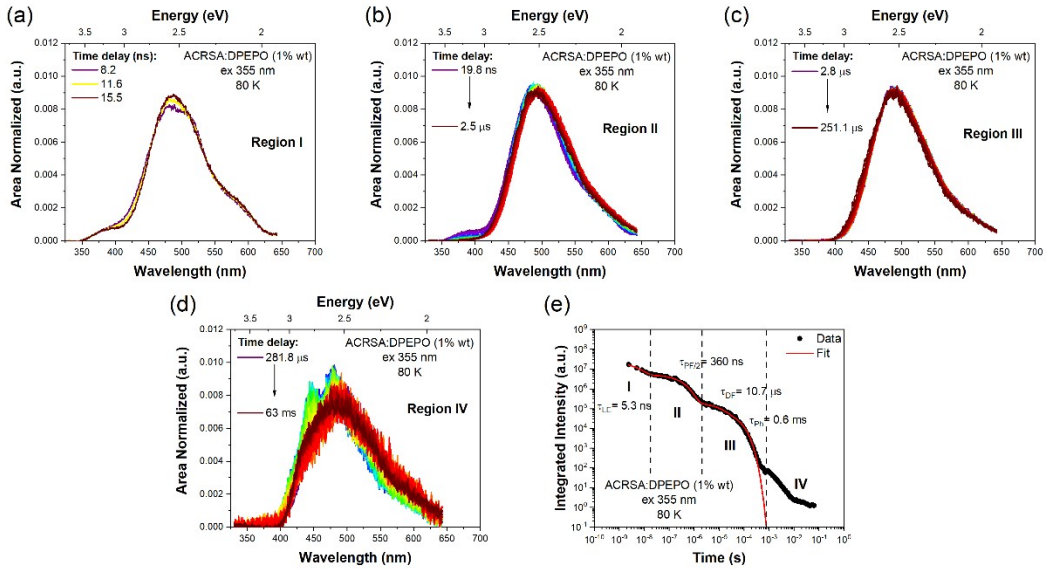

Figure S7. (a)-(d) Area normalised time resolved spectra ACRSA in DPEPO (1% wt), shown in the four main regimes indicated in (e). (e) Fitting of kinetic decay results at 80 K. Laser excitation at 355 nm. Data is tabulated in **Table S2**.

8. Fittings of kinetic decay results of ACRSA:Zeonex (1%wt loading) at room temperature, with 337 nm excitation wavelength:

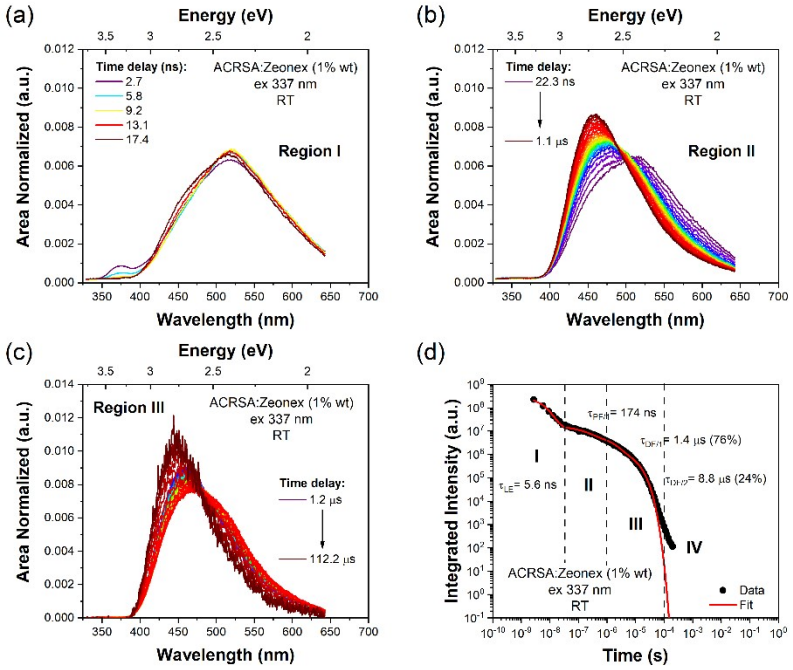

Figure S8. (a)-(c) Area normalised time resolved spectra of ACRSA in zeonex (1% wt), shown in the three main regimes indicated in (d). (d) Fitting of kinetic decay results at room temperature. Laser excitation at 337 nm. Data is tabulated in **Table S1**.

9. Lifetime and rates obtained from data fitting of ACRSA in Zeonex (1%), UGH, DPEPO (1% and 10%) and neat film measured at room temperature, with 337 nm excitation wavelength.

Table S1. Lifetime and amplitude results from data fitting of ACRSA in zeonex (1%), UGH, DPEPO (1% and 10%) and neat film measured at 300 K; with 337 nm excitation wavelength.

ACRSA:HOST	Zeonex 1%	DPEPO 1%	UGH 1%	DPEPO 10%	UGH 10%	NEAT
τ_{LE} (ns)	5.6	4.5	4.8	14.6	7.3	23.9
$\tau_{PF/1}$ (ns)/ $A_{PF/1}$ (%)	174	202	87.3	95.9/68	64.5/66	119/80
$\tau_{PF/2}$ (ns)/ $A_{PF/2}$ (%)	-	-	-	307/32	295/34	586/20
$\tau_{DF/1}$ (µs)/ $A_{DF/1}$ (%)	1.4/76	-	-	-	-	-
$\tau_{DF/2}$ (µs)/ $A_{DF/2}$ (%)	8.8/24	7.8	5.0	8.3	6.6	8.3
$\tau_{AV/PF}$ (ns)	174	202	87.3	223	226	375
$\tau_{AV/DF}$ (µs)	6.3	7.8	5.0	7.72	6.6	8.3
k_{rad} (s^{-1}) x10^6	1.04	0.70	0.93	1.23	1.33	3.08
k_{ISC} (s^{-1}) x10^6	4.69	4.25	10.5	9.19	14.2	5.30
k_{rISC} (s^{-1}) x10^6	3.79	0.90	2.45	1.02	1.76	0.35

10. Fittings of kinetic decay results of ACRSA:Zeonex (0.01%wt loading) at room temperature, with 355 nm excitation wavelength:

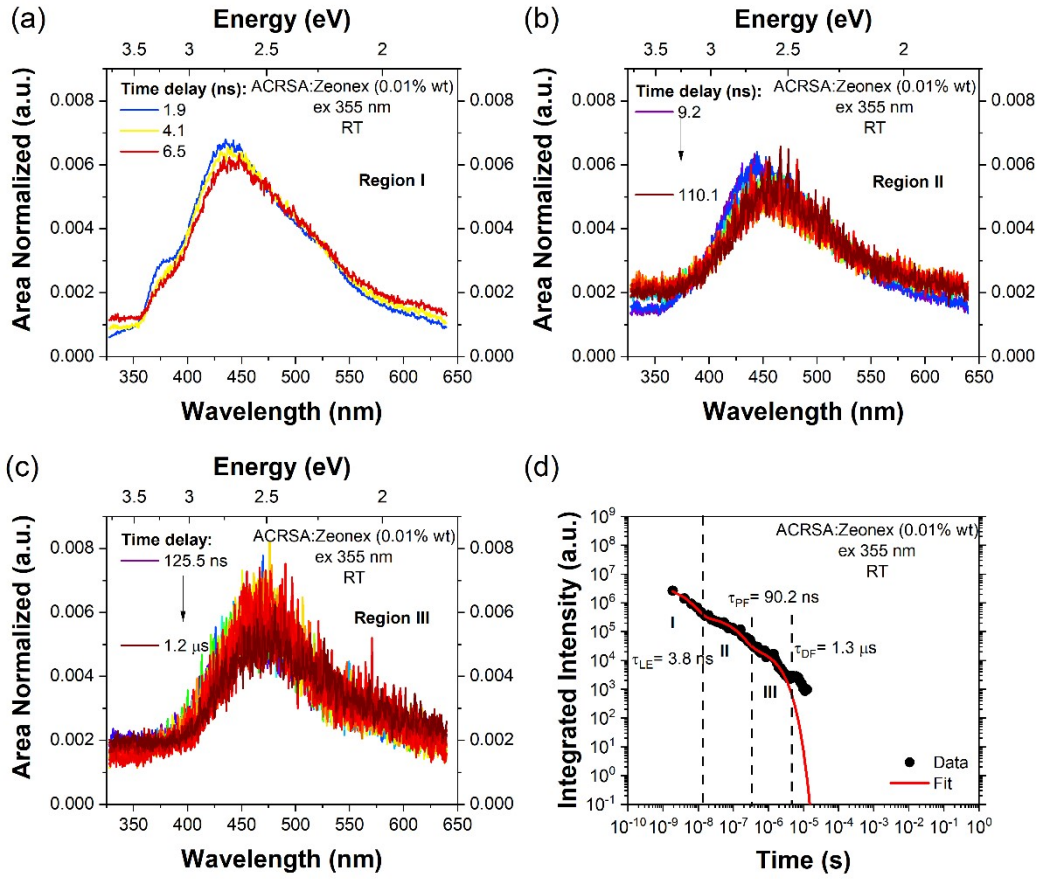

Figure S9 *(*a)-(c) Area normalised time resolved spectra for highly diluted ACRSA (0.01%) in zeonex shown in the three main regimes indicated in (d). (d) Fitting of kinetic decay results at 300 K. Laser excitation at 355 nm. At such high dilution, it is clear that both 1LE and 1CT emission species are present but there is no 550 nm species, which we therefore attribute to an intermolecular species.

11. Fittings of kinetic decay results of ACRSA in UGH and DPEPO (1%wt loading) at room temperature, with 355 nm excitation wavelength:

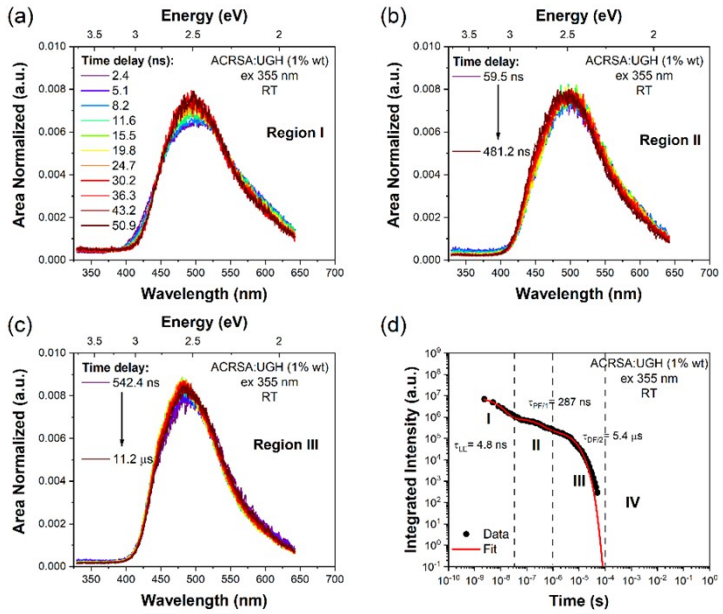

Figure S10. (a)-(c) Area normalised time resolved spectra of ACRSA in UGH (1% wt), shown in the three main regimes indicated in (d). (d) Fitting of kinetic decay results at room temperature. Laser excitation at 355 nm. Data is tabulated in **Table 1**.

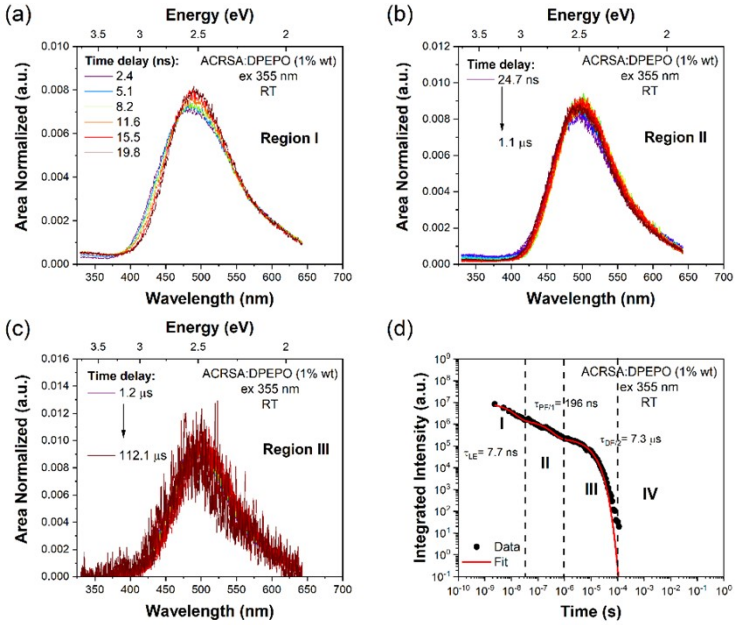

Figure S11. (a)-(c) Area normalised time resolved spectra of ACRSA in DPEPO (1% wt), shown in the three main regimes indicated in (d). (d) Fitting of kinetic decay results at room temperature. Laser excitation at 355 nm. Data is tabulated in **Table 1**.

12. Excitation dependent steady state measurements of 10%wt loading and neat films:

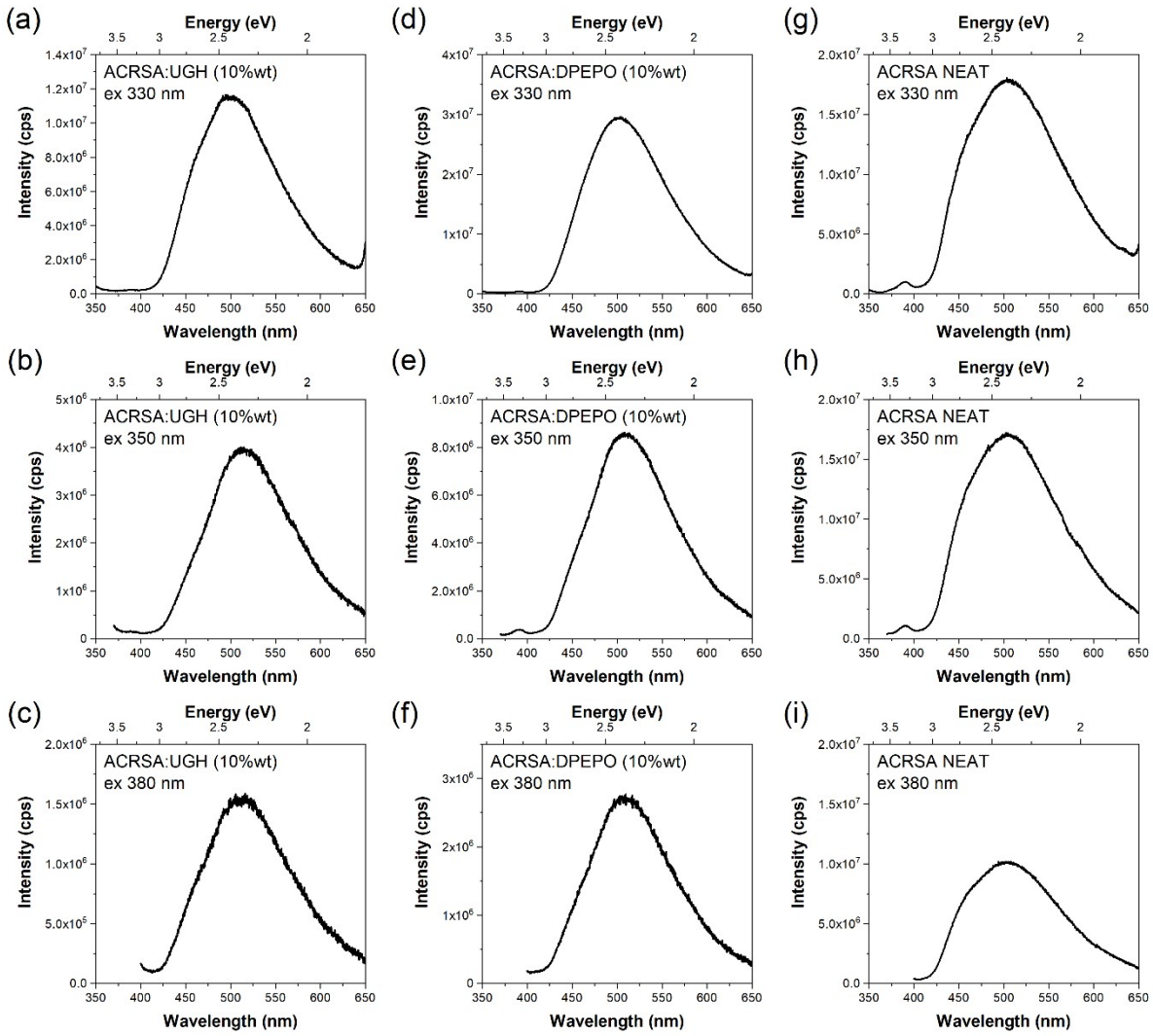

Figure S12. Excitation wavelength dependent steady state emission from ACRSA dispersed in UGH (a-c), DPEPO host (d-f) at 10%wt loading and neat (g-i) films, measured at room temperature in air.

13. Fittings of kinetic decay results of ACRSA in UGH, DPEPO (10% loading) and neat films at room temperature, with 355 nm excitation wavelength:

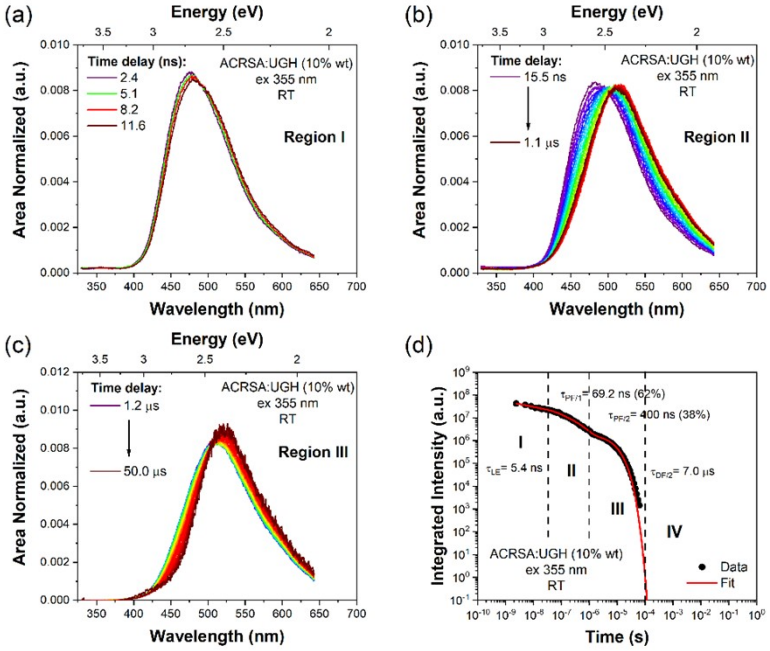

Figure S13. (a)-(c) Area normalised time resolved spectra of ACRSA in UGH (10% wt), shown in the three main regimes indicated in (d). (d) Fitting of kinetic decay results at room temperature. Laser excitation at 355 nm. Data is tabulated in **Table 1**.

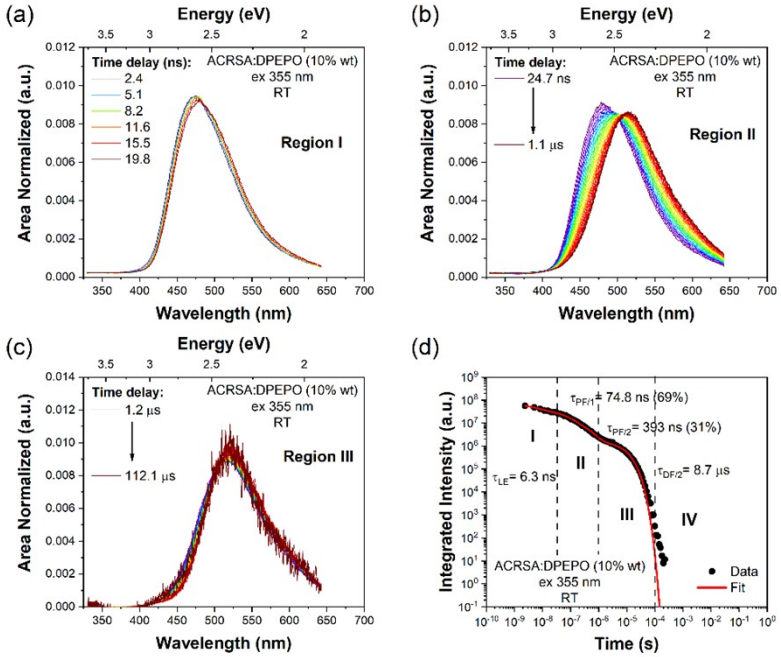

Figure S14. (a)-(c) Area normalised time resolved spectra of ACRSA in DPEPO (10% wt), shown in the three main regimes indicated in (d). (d) Fitting of kinetic decay results at room temperature. Laser excitation at 355 nm. Data is tabulated in **Table 1**.

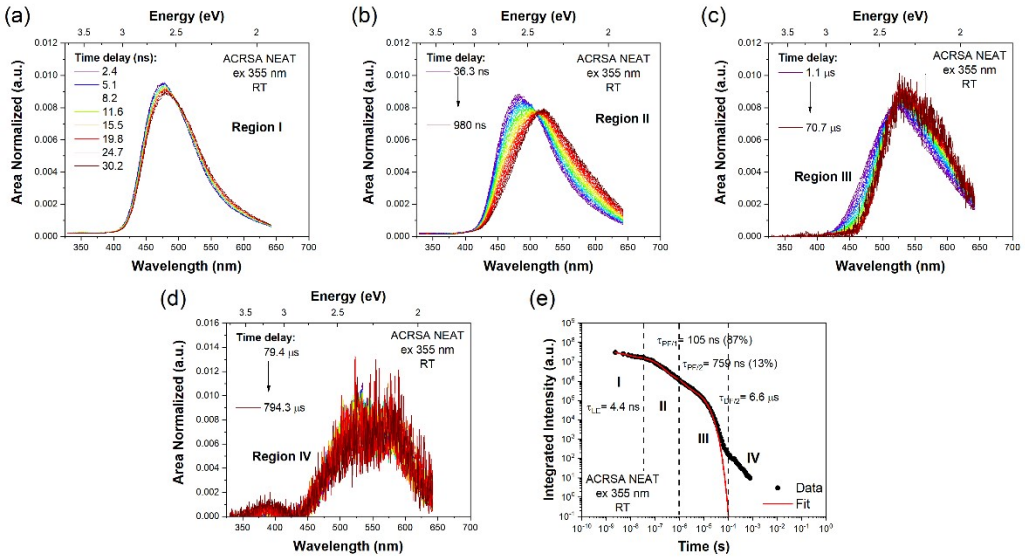

Figure S15. (a)-(d) Area normalised time resolved spectra of neat film, shown in the four main regimes indicated in (e). (e) Fitting of kinetic decay results at room temperature. Laser excitation at 355 nm. Data is tabulated in **Table 1**.

14. Lifetimes obtained from data fitting of ACRSA in Zeonex (1%), UGH, DPEPO (1% and 10%) and neat film measured at 80 K, with 355 nm excitation wavelength.

Table S2. Lifetime and amplitude results from data fitting of ACRSA in Zeonex (1%), UGH, DPEPO (1% and 10%) and neat film measured at 80 K; with 355 nm excitation wavelength.

ACRSA:HOST	Zeonex 1%	DPEPO 1%	UGH 1%	DPEPO 10%	UGH 10%	NEAT
τ_{LE} (ns)	14.5	5.3	4.7	-	10.1	-
$\tau_{PF/1}$ (ns)/ $A_{PF/1}$ (%)	67.1/85	-	-	97.8/69	-	70.9/71
$\tau_{PF/2}$ (ns)/ $A_{PF/2}$ (%)	456/15	360	439	745/31	391	438/29
τ_{DF} (μs)/ A_{DF} (%)	9.4	10.7	7.7	9.2	7.1	7.4
τ_{Ph} (ms)/ A_{Ph} (%)	1.0	0.6	0.7	0.7	0.7	0.5

15. Fittings of kinetic decay results of ACRSA in UGH, DPEPO (10% loading) and neat films at 80 K, with 355 nm excitation wavelength:

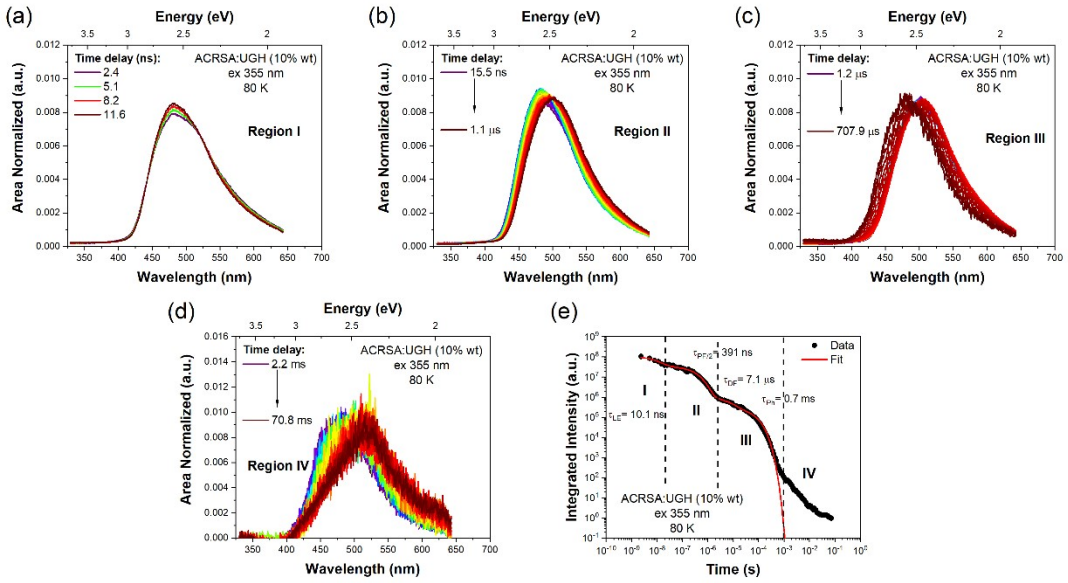

Figure S16. (a)-(d) Area normalised time resolved spectra of ACRSA in UGH (10% wt), shown in the four main regimes indicated in (e). (e) Fitting of kinetic decay results at 80 K. Laser excitation at 355 nm. Data is tabulated in **Table S2**.

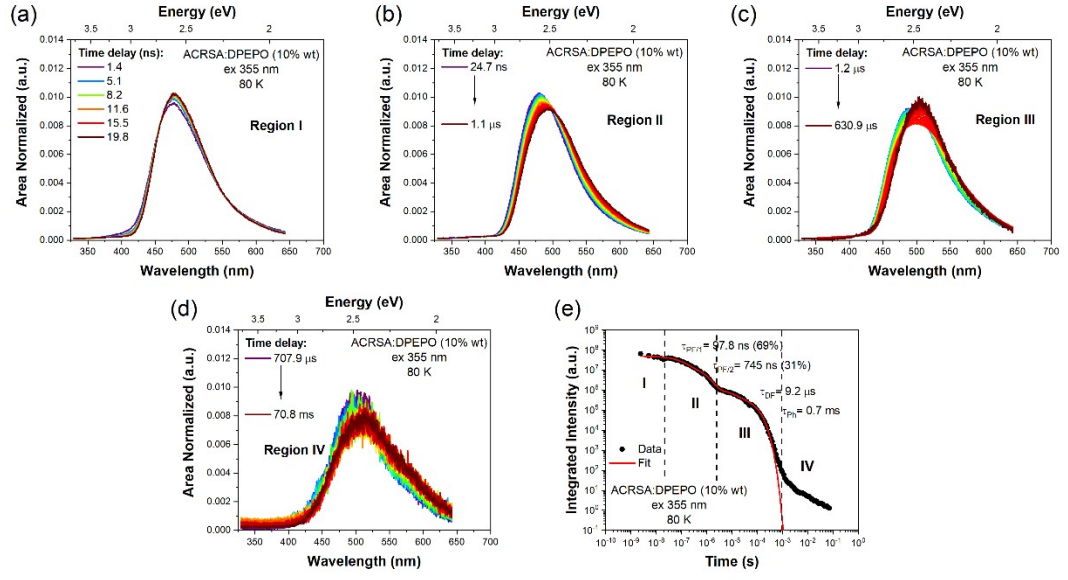

Figure S17. (a)-(d) Area normalised time resolved spectra of ACRSA in DPEPO (10% wt), shown in the four main regimes indicated in (e). (e) Fitting of kinetic decay results at 80 K. Laser excitation at 355 nm. Data is tabulated in **Table S2**.

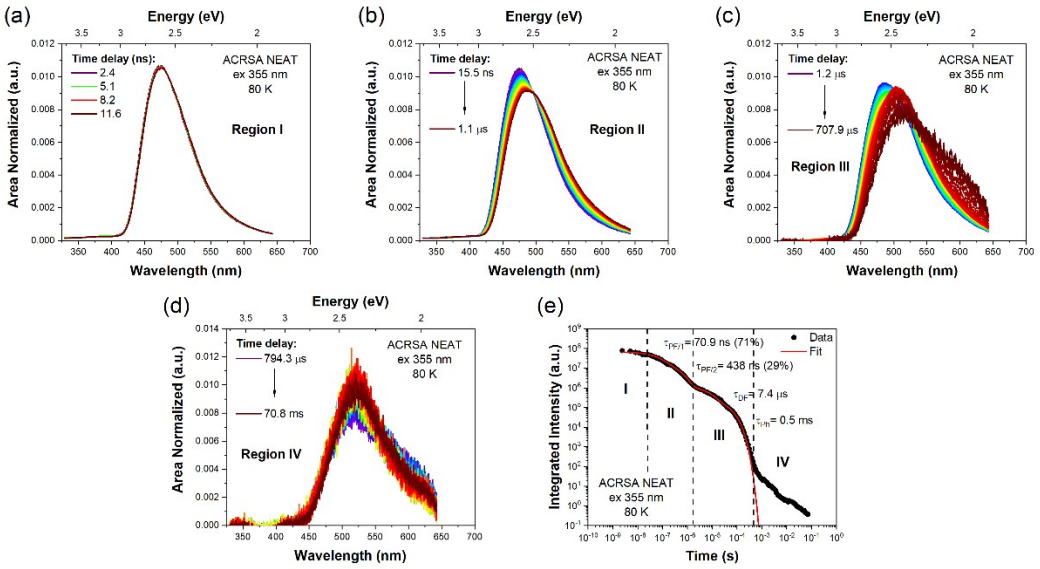

Figure S18. (a)-(d) Area normalised time resolved spectra of neat film, shown in the four main regimes indicated in (e). (e) Fitting of kinetic decay results at 80 K. Laser excitation at 355 nm. Data is tabulated in **Table S2**.

16. Scaled kinetic traces to film absorbance of ACRSA at 1% and 10% wt loading in UGH and DPEPO host matrices

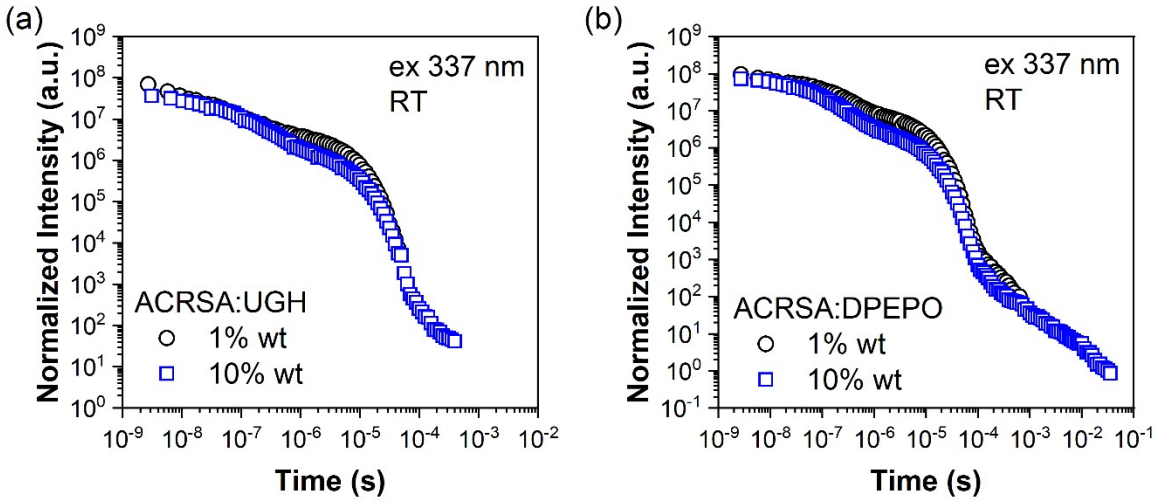

Figure S19. Scaled kinetic traces to film absorbance showing quenching of the prompt emission at 10% loading and hence less DF contribution, indicative of the presence of dimer/excimer states in the higher loaded films.

17. Power dependence results

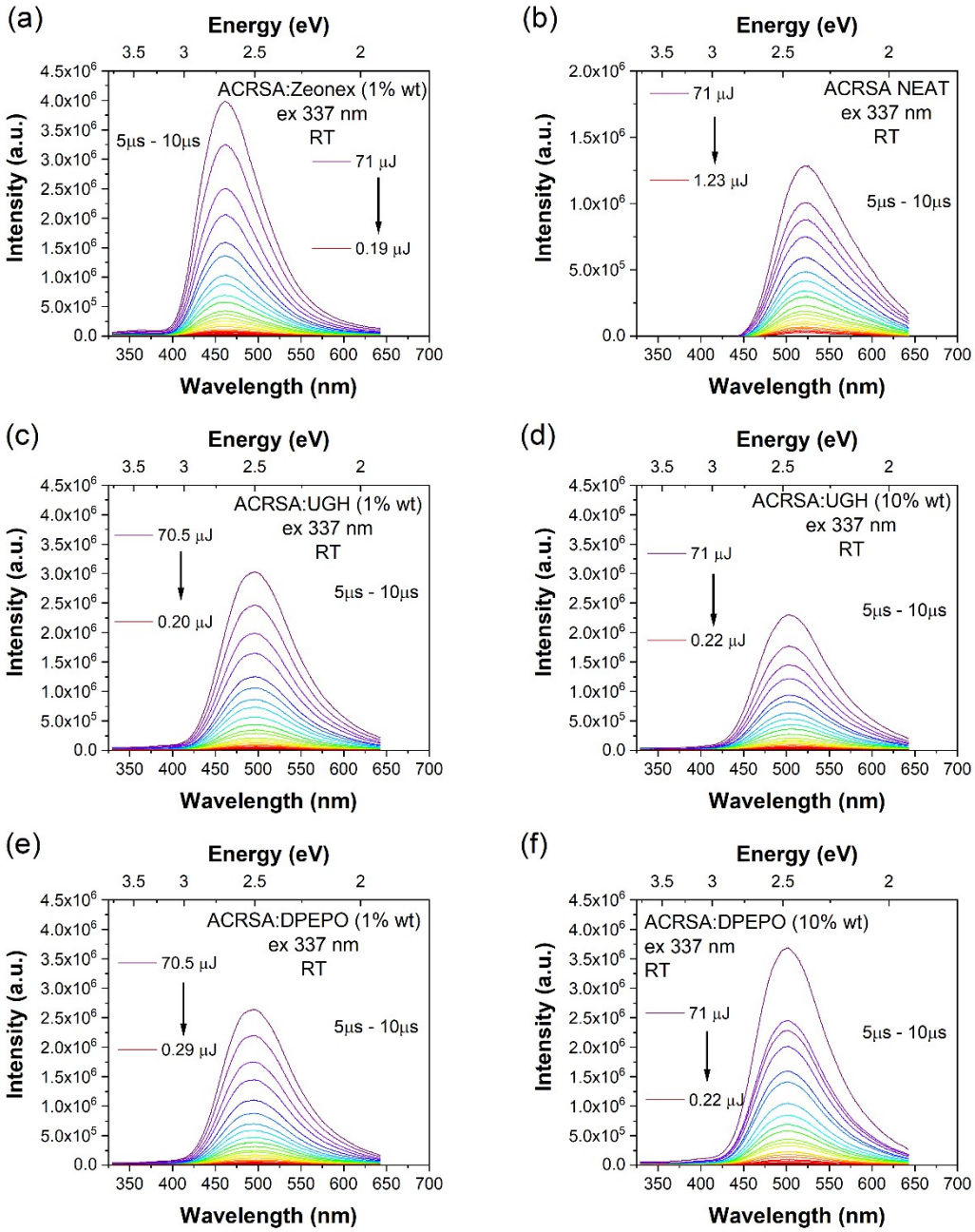

Figure S20. Power dependence of delayed fluorescence spectra of ACRSA in different host matrices at 1% and 10% loading, recorded at room temperature.

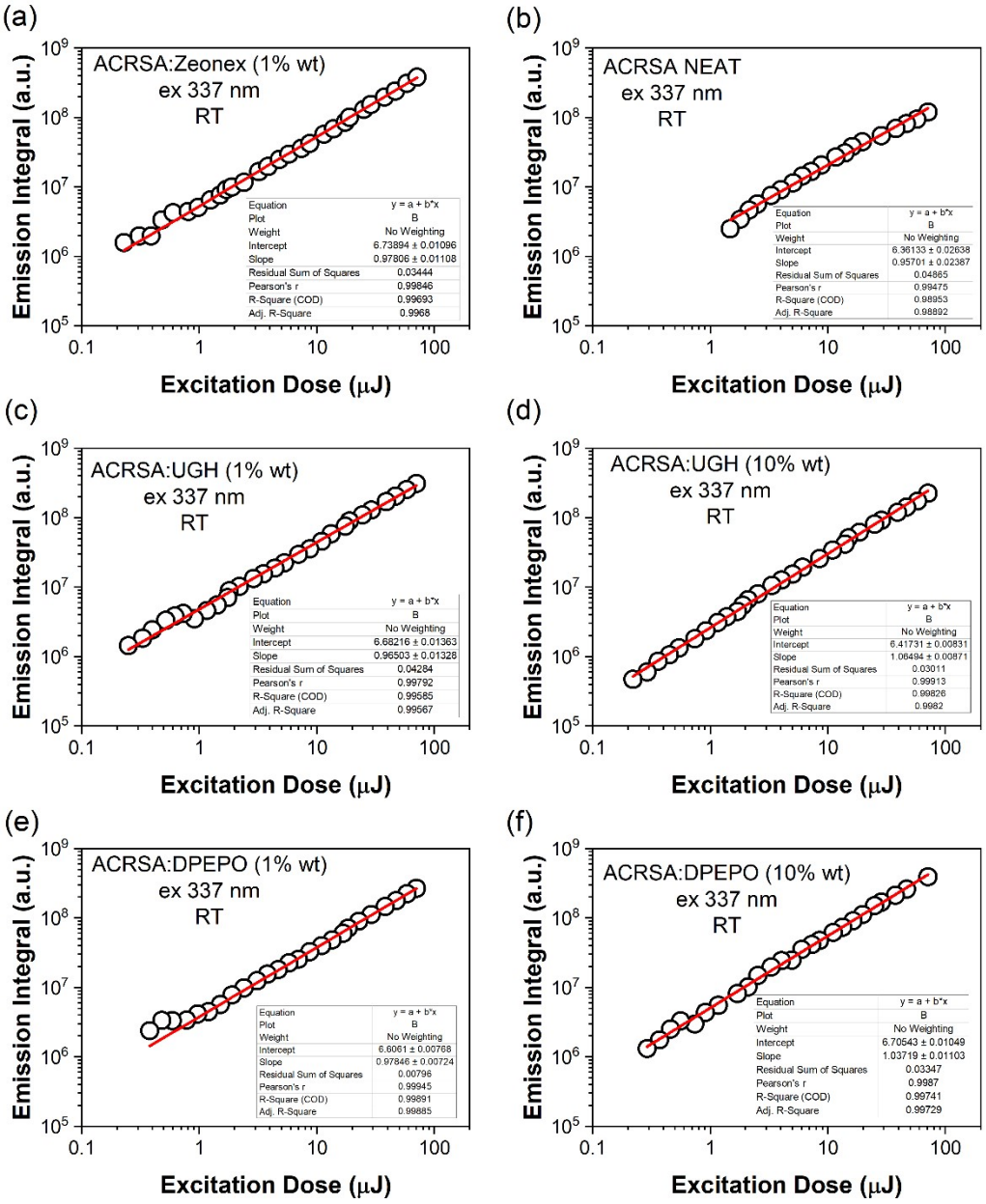

Figure S21. Linear fit of the DF intensity as a function of excitation power for ACRSA in different host matrices at 1% and 10% loading, recorded at room temperature.

18. X-ray structure of ACRSA

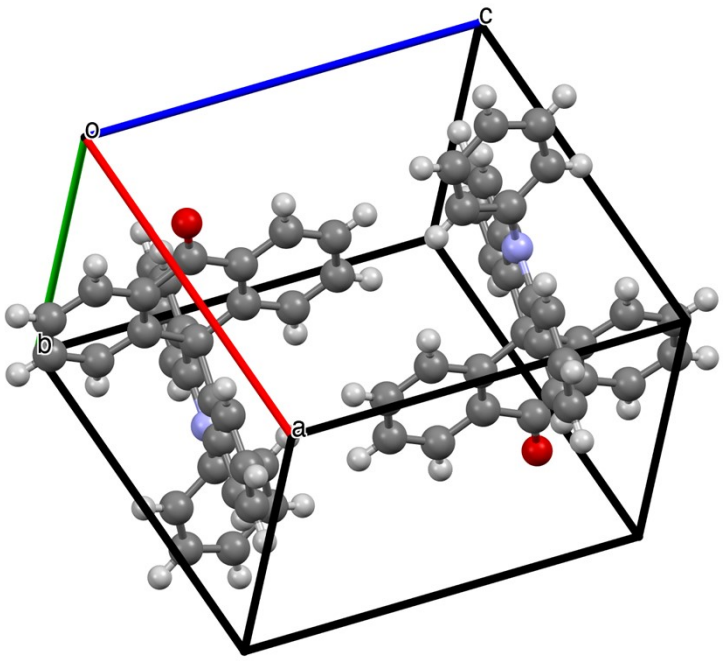

Figure S22. X-ray structure of ACRSA showing the high degree of orthogonality between the donor and acceptor units. We also observe partial face to face overlap of the acceptor units. X-ray data very kindly supplied by Prof Adachi.

19. Normalised time resolved emission spectra:

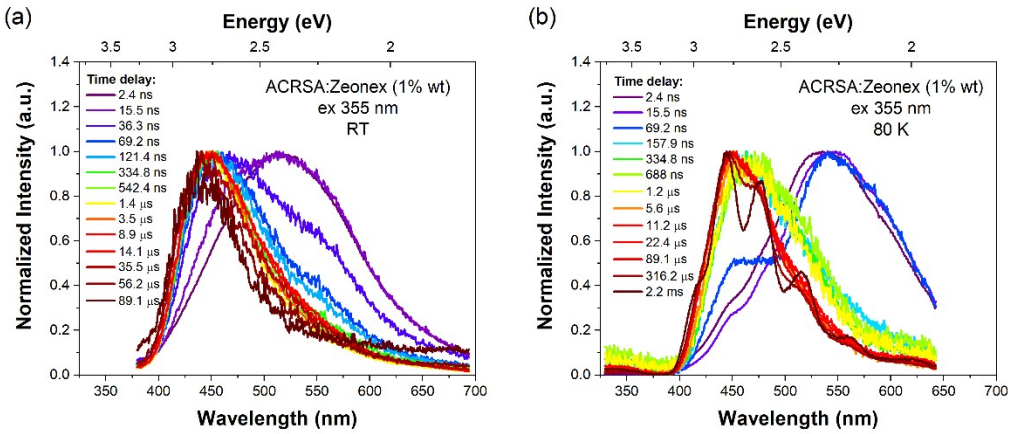

Figure S23. Time evolution of the emission spectra (normalised intensity) for ACRSA in zeonex (1% loading) measured at (a) 300 K and (b) 80 K. Laser excitation at 355 nm excitation wavelength.

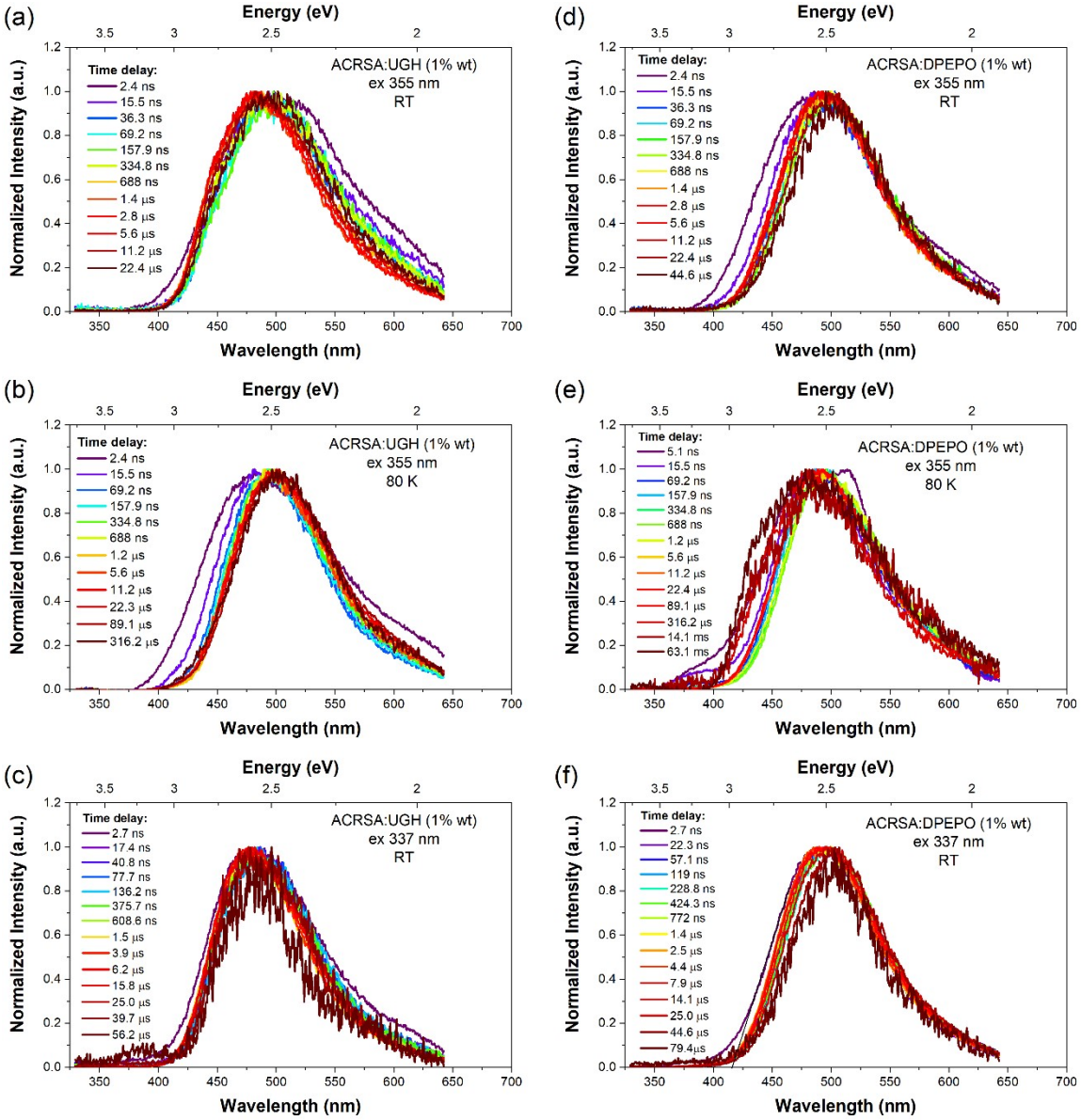

Figure S24. Guest concentration dependence on the time dependent emission spectra of ACRSA (normalised intensity). Time resolved emission spectra from ACRSA at 1% loading in UGH and DPEPO host matrices, measured at room temperature and 80 K, with 355 nm and 337 nm excitation.

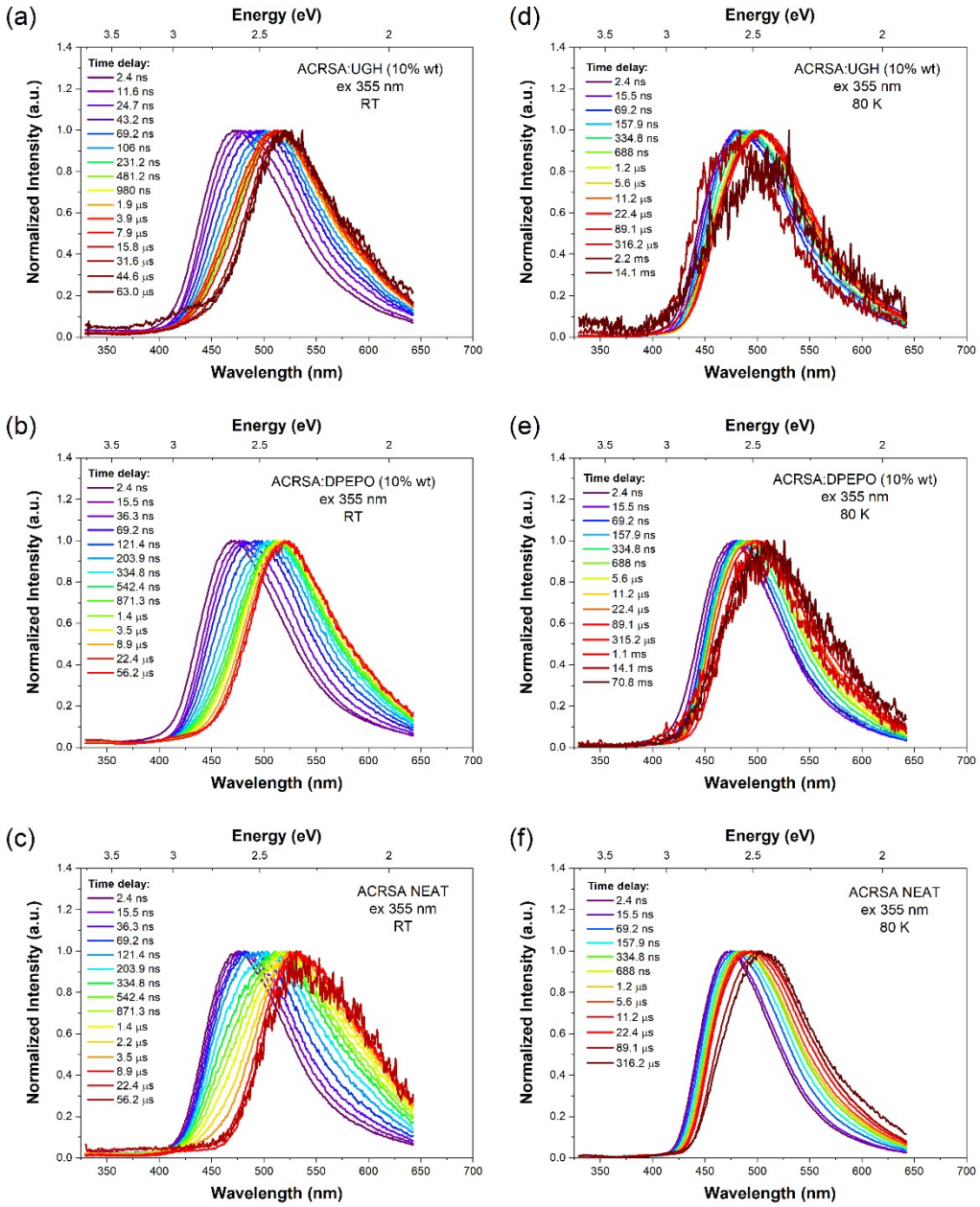

Figure S25. Time evolution of the emission spectra (normalised intensity). Laser excitation at 355 nm excitation wavelength, for ACRSA in UGH, DPEPO (10% loading) and neat film measured at; (a-c) 300 K, (d-f) at 80 K.

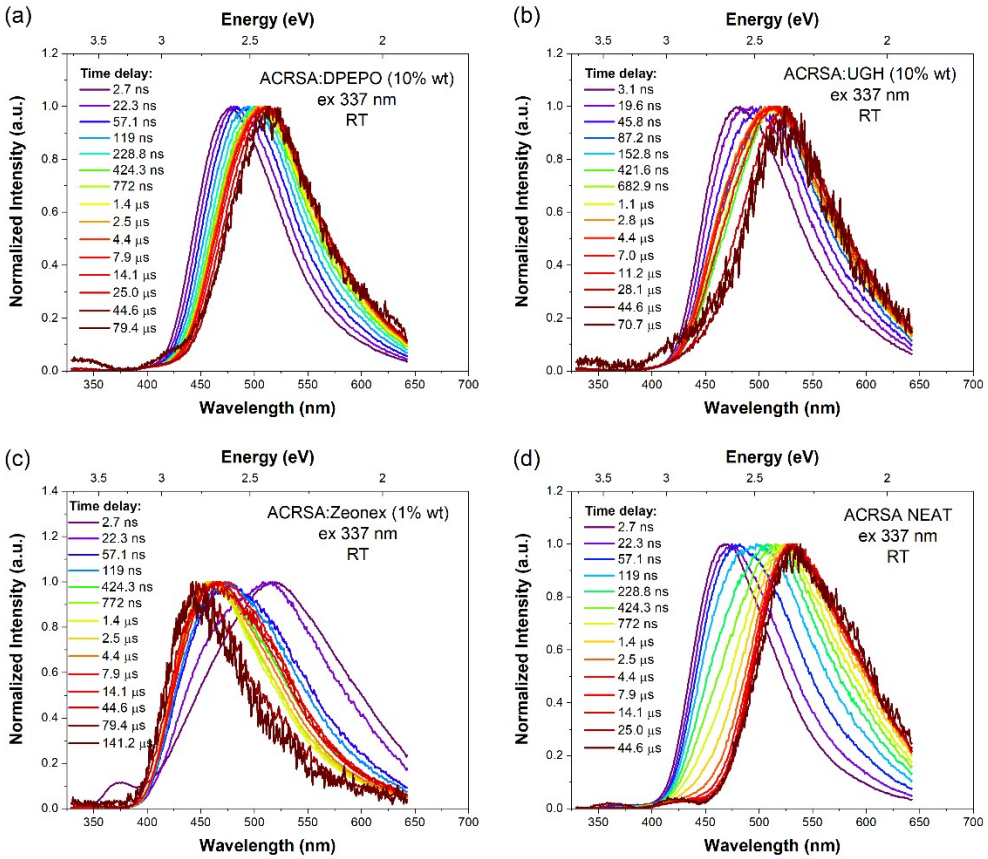

Figure S26. Time evolution of the emission spectra (normalised intensity). Laser excitation at 337 nm excitation wavelength, for ACRSA in (a) DPEPO, (b) UGH (10% loading), (c) zeonex (1% loading) and (d) neat film measured at room temperature.

20. Emission decay kinetics for ACRSA films

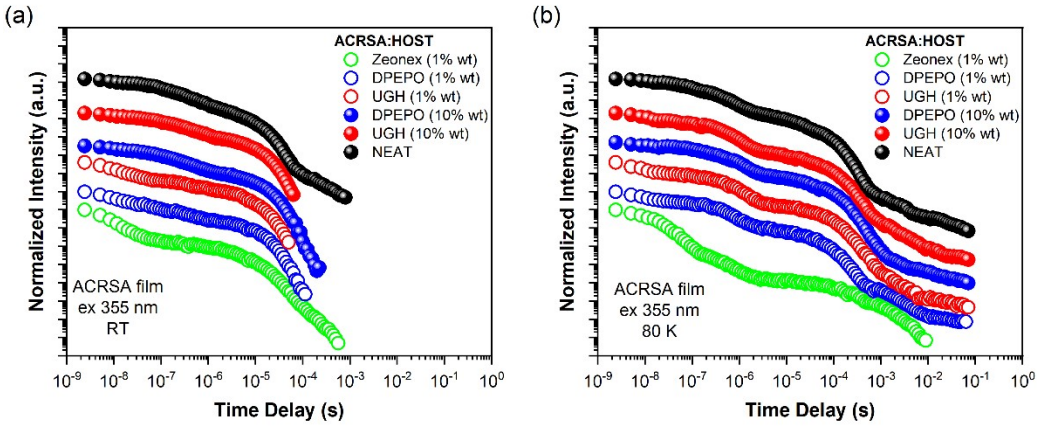

Figure S27. Temperature dependent emission decay kinetics for ACRSA films. Time resolved emission decay for ACRSA in different host matrices, recorded at (a) 300 K and (b) 80 K. Laser excitation at 355 nm.

21. Results and discussion of time resolved emission spectra, with 337 nm excitation wavelength.

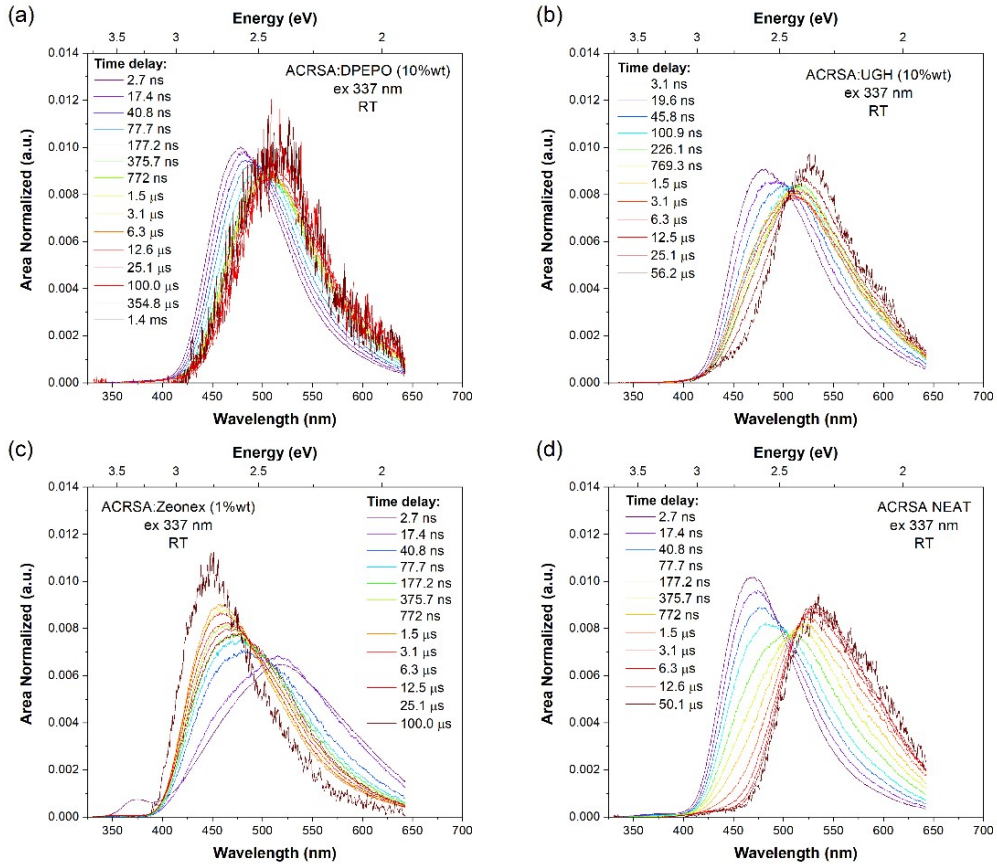

Figure S28. Time evolution of the emission spectra (area normalised). Laser excitation at 337 nm excitation wavelength, for ACRSA in DPEPO, UGH (10% loading), zeonex (1% loading), and neat film measured at; (a-d) 300 K. Normalised data shown in **Figure S26**.

Turning to measurements made using 337 nm excitation, **Figure S28 a-d**, which excites the 1^1B_1 donor exciton state. At 300 K in UGH, DPEPO and neat films, we observe very similar photophysics as with 355 nm excitation. Detailed time resolved spectra are given in **Figure S29-S33**, and decay times given in **Table S1**.

In zeonex, we observe complex, fast (in our first few time windows) emission at 350-400 nm (peak at 370 nm) which we previously observed in solution state measurements and assigned to emission from the 1^1B_1 bright donor exciton state (which has very strong absorption at 337 nm) and a shoulder at 395 nm (3.14 eV) which is a signature of the fast emitting ^{1}LE acceptor

local state. Again, we also observe a very broad highly red shifted Gaussian feature centred at 520 nm (2.38 eV) which decays faster with 337 nm than 355 nm excitation. After this initial fast time period, we observe the evolution of two emitting CT bands, with an isoemissive point at ca. 490 nm in the area normalised data, having lifetimes of 1.4 μs and 8.8 μs, similar decay to those measured with 355 nm excitation, but now clearly showing two resolved emission bands. The red component has a much longer lifetime. This redder CT band matches well to the CT band observed in DPEPO (1% loading, see **Figure 3**) whereas the bluer one matches that seen in zeonex with 355 nm excitation, ascribed to the LE/CT mixed state. We can only really speculate as to the origin of the redder band, but from it's spectral position we think it could be from remnant molecules with distorted conformation that are hindered by the matrix from reverting back to the lowest energy molecular conformation. In general, 337 nm excitation gives slightly broader spectra indicative of the greater excess energy allowing more molecular conformations to be accessed along with hot state (vibrationally unrelaxed) emission which blurs the vibronic structure of bands, as described previously by Greene *et al*[5].

22. Fittings of kinetic decay results of ACRSA in UGH, DPEPO (1% and 10% wt loading) and neat film at room temperature, with 337 nm excitation wavelength:

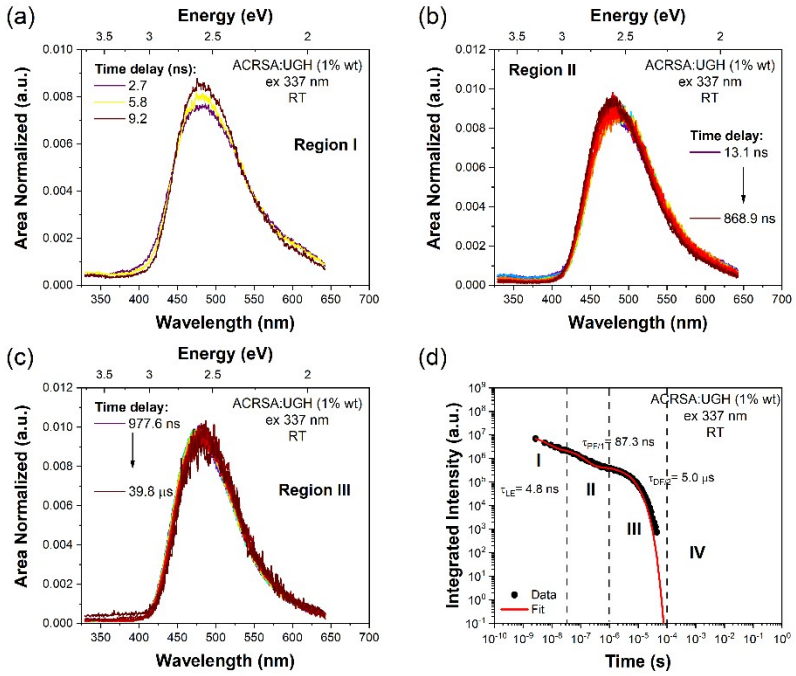

Figure S29. (a)-(c) Area normalised time resolved spectra of ACRSA in UGH (1% wt), shown in the three main regimes indicated in (d). (d) Fitting of kinetic decay results at room temperature. Laser excitation at 337 nm. Data is tabulated in **Table S1**.

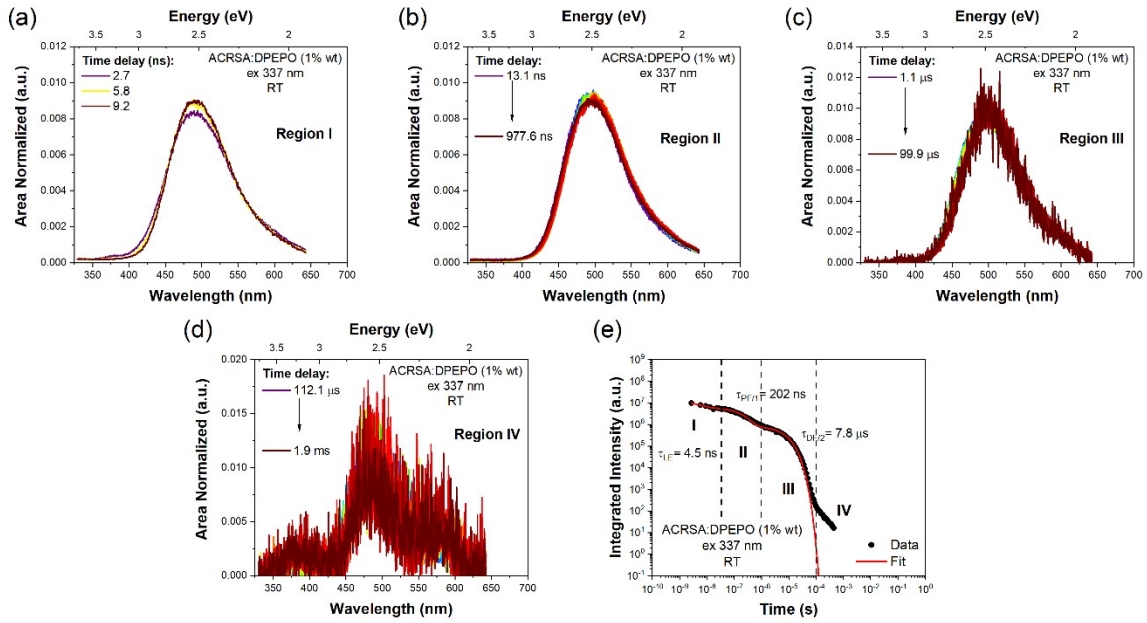

Figure S30. (a)-(d) Area normalised time resolved spectra of ACRSA in DPEPO (1% wt), shown in the four main regimes indicated in (e). (e) Fitting of kinetic decay results at room temperature. Laser excitation at 337 nm. Data is tabulated in **Table S1**.

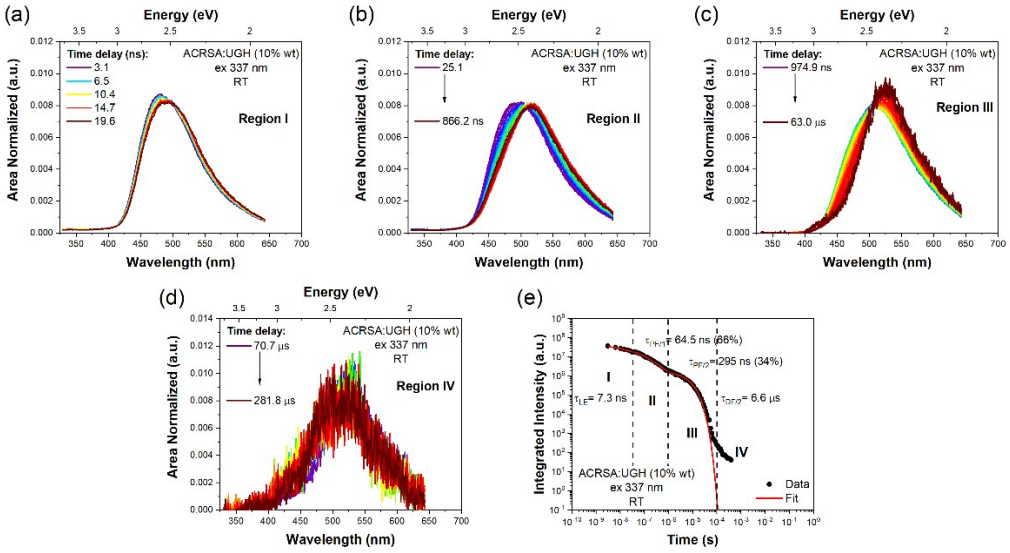

Figure S31. (a)-(d) Area normalised time resolved spectra of ACRSA in UGH (10% wt), shown in the four main regimes indicated in (e). (e) Fitting of kinetic decay results at room temperature. Laser excitation at 337 nm. Data is tabulated in **Table S1**.

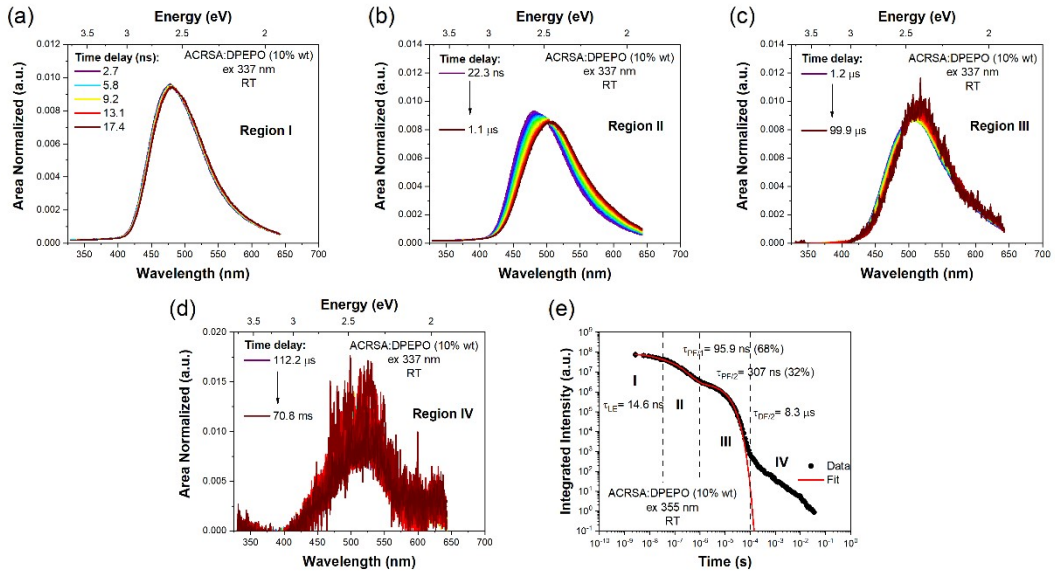

Figure S32. (a)-(d) Area normalised time resolved spectra of ACRSA in DPEPO (10% wt), shown in the four main regimes indicated in (e). (e) Fitting of kinetic decay results at room temperature. Laser excitation at 337 nm. Data is tabulated in **Table S1**.

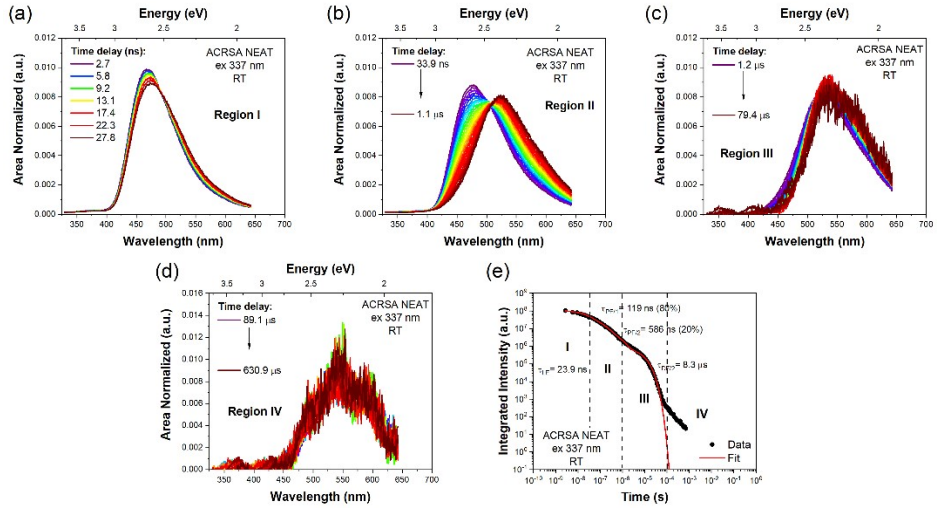

Figure S33. (a)-(d) Area normalised time resolved spectra of neat film, shown in the four main regimes indicated in (e). (e) Fitting of kinetic decay results at room temperature. Laser excitation at 337 nm. Data is tabulated in **Table S1**.

23. References

(1) Franca, L. G.; Long, Y.; Li, C.; Danos, A.; Monkman, A. The Critical Role of Nπ* States in the Photophysics and Thermally Activated Delayed Fluorescence of Spiro Acridine-Anthracenone. *J. Phys. Chem. Lett.* **2021**, *12* (5), 1490–1500. https://doi.org/10.1021/acs.jpclett.0c03314.

(2) Lyskov, I.; Marian, C. M. Climbing up the Ladder: Intermediate Triplet States Promote the Reverse Intersystem Crossing in the Efficient TADF Emitter ACRSA. *J. Phys. Chem. C* **2017**, *121* (39), 21145–21153. https://doi.org/10.1021/acs.jpcc.7b06187.

(3) Penfold, T. J.; Dias, F. B.; Monkman, A. P. The Theory of Thermally Activated Delayed Fluorescence for Organic Light Emitting Diodes. *Chem. Commun.* **2018**, *54* (32), 3926–3935. https://doi.org/10.1039/c7cc09612g.

(4) Gibson, J.; Monkman, A. P.; Penfold, T. J. The Importance of Vibronic Coupling for Efficient Reverse Intersystem Crossing in Thermally Activated Delayed Fluorescence Molecules. *ChemPhysChem* **2016**, *17* (19), 2956–2961. https://doi.org/10.1002/cphc.201600662.

(5) Greene, B. I.; Hochstrasser, R. M.; Weisman, R. B. Picosecond Transient Spectroscopy of Molecules in Solution. *J. Chem. Phys.* **1979**, *70* (3), 1247–1259. https://doi.org/10.1063/1.437617.